Numerical analysis and experimental characterization of broadly tunable erbium doped fiber ring laser

QI WANG*, YONG ZHAO, YUYAN ZHANG, YA'NAN ZHANG, BO HAN
Northeastern University, College of Information Science and Engineering, P. O. Box 321, Shenyang, Liaoning, 110819, China

The output power characteristics of a wideband tunable erbium-doped fiber ring laser (EDFRL) are studied through numerical analysis and experiments. A numerical model based on an iterative solution of propagation rate equations is established to analyze the influence of total intracavity loss, erbium-doped fiber length and output couple ratio on the output power characteristics of EDFRL. The numerical results are in good agreement with the experimentally obtained data. Both the numerical analysis and experimental results show that minimization of the intra-cavity loss as well as optimization of the erbium-doped fiber length and the selection of a appropriate output coupling ratio are the same important for achieving high output power, well power stability, output spectrum flatness and output bandwidth. A 147 nm tunable range which covering the whole S+C+L band is achieved in the experiments. This fiber ring laser has a flat, stable output spectrum and better than 62 dB signal-to-ASE-noise ratio.

(Received March 24, 2011; accepted May 25, 2011)

Keywords: Fiber optics, Numerical modeling, Lasers, Erbium-doped fiber, Tunable lasers

1. Introduction

During the past decade, wavelength tunable erbium-doped fiber lasers have attracted much research interest along with the development of erbium doped fiber amplifiers and fiber lasers technologies not only for its potential use in high-bandwidth fiber-optic communication, spectroscopy, sensing, but also crucial to bio-photonic applications such as optical coherence tomography (OCT) and laser orthopedic surgery. Wavelength tunable erbium-doped fiber lasers become attractive also for its unique characteristics such that low threshold, high optical signal-to noise ratio (OSNR), wide frequency band, high output power, narrow linewidth, compatible with the fiber optic components. At the same time, along with the development of related technologies, widely tunable erbium-doped fiber lasers (EDFLs) have been studied extensively for applications related to gas sensors, high-resolution spectroscopy, and fiber optic communications, particularly for performance testing of optical fiber components for CWDM networks. In recent years, tunable EDFLs pumped with a 980 nm semiconductor laser diode have been demonstrated with continuously tuning range of 80 nm (1520–1600 nm) by Yamashita *et al* [1] and over 100 nm by Antoine Bellemare *et al* [2-4]. Different theoretical models have been presented in the aforementioned works to analyze laser performance but none of them has considered all the parameters simultaneously. This makes it difficult to predict the laser performance and to optimize the laser design.

In this paper, based on an iterative solution of the propagation-rate equations of a two-level laser system, we present a comprehensive theoretical model for the EDFRLs. The model is used to analyze the output power characteristics of the EDFRLs as a function of emission wavelength, the total intracavity loss, output coupling ratio, and active fiber length, etc. Based on the analysis, a broadband tunable silica-based EDFRL that can be continuously tuned about 147 nm covering the whole S and C+L bands from 1479 nm to 1616 nm is demonstrated experimentally. To our knowledge, the experimental results concerning this laser show the widest tuning range (over 147 nm) ever reported for an erbium-doped fiber laser [5-9].

2. Experimental setup

Fig. 1 shows the configuration of the wideband wavelength tunable erbium-doped fiber ring laser. The gain media of the laser is a length of standard silica-based C-band erbium-doped fiber (EDF). The EDF is backward pumped by a 200 mW laser diode (LD) emitting at 980 nm through a 980/1550 nm microoptic WDM coupler. Two optical isolators (ISO) are inserted in the ring cavity to guarantee unidirectional laser operation and prevent back reflections to enhance laser power stability. Forward ASE

generated from EDF propagate through the FFP-TF and output coupler, 10% of light output as laser and the other propagate in the ring cavity. The output is observed using an optical spectrum analyzer (OSA, ANDO AQ6317C) of 0.02 nm resolution.

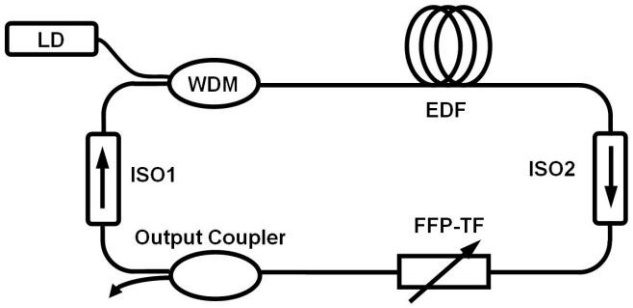

Fig. 1. Schematic diagram of the wideband tunable erbium-doped fiber ring laser.

A fiber Fabry-Perot tunable filter (FFP-TF) is one of the most suitable tunable filters for wavelength tunable lasers because it has a wide tuning range (over 100 nm) and fast switching speed (several microseconds). The FFP-TF (Micron optics Inc. MOI) used in the configuration as the laser wavelength selection component is an all-fiber device with an insertion loss of 2.2 dB, polarization dependent loss (PDL) of 0.13 dB, 3 dB bandwidth of 0.162 nm, the FFP-TF with a finesse of 639 and a free spectral range (FSR) of 173 nm. The FSR of the FFP-TF can be further extended when higher driving voltage is applied. The estimated total intracavity loss of the laser configuration is about 3 dB.

3. Theoretical model and numerical simulation

The theoretical model is based on a homogeneously broadened two-level approximation of an erbium ion [10]. In the case of 980 nm LD pumping, the upper pump level is assumed to be unpopulated, and the atomic population densities n_1, n_2 (averaged over EDF cross section) at the ground and metastable energy levels ${}^4I_{15/4}$, ${}^4I_{13/4}$ are given by the steady-state rate equations [11]:

$$\frac{dn_1(z,t)}{dt} = -[W_a(z)+W_p(z)]n_1(z,t)+[W_e(z)+\frac{1}{\tau_{21}}]n_2(z,t)$$

$$\frac{dn_2(z,t)}{dt} = -[W_e(z)+\frac{1}{\tau_{21}}]n_2(z,t)+[W_a(z)+W_p(z)]n_1(z,t)$$

Where τ_{21} is the spontaneous emission lifetime of the metastable level. W_p, W_a and W_e are the pumping, stimulated absorption and stimulated emission rates, respectively.

$$W_a(z) = \frac{1}{A_{eff}}\int_0^\infty \frac{\sigma_a(\upsilon)}{h\upsilon}[P_{ASE+}(z,\upsilon)+P_{ASE-}(z,\upsilon)]\eta(\upsilon)d\upsilon$$

$$W_e(z) = \sigma_e(\upsilon_p)\frac{P_p(z)}{h\upsilon_p A_{eff}}\eta_p + \frac{1}{A_{eff}}\int_0^\infty \frac{\sigma_e(\upsilon)}{h\upsilon}[P_{ASE+}(z,\upsilon)+P_{ASE-}(z,\upsilon)]\eta(\upsilon)d\upsilon$$

$$W_P(z) = \sigma_a(\upsilon_p)\frac{P_P(z)}{h\upsilon_p A_{eff}}\eta_p$$

In these equations, σ_a, σ_e are the appropriate emission/absorption cross sections, h is Planck's constant, $P_p(z)$ and $P^{\pm}_{ASE}(z,\upsilon)$ are the pump powers and ASE powers at frequency in a frequency interval and at the longitudinal fiber coordinate respectively. A_{eff} is the effective fiber core area, $\eta(\upsilon)$ are the overlap integrals between the LP mode intensity distribution and the erbium doping density function $\rho(r)$,

$$\eta(\upsilon) = \frac{\int_0^\infty \rho(r)\left|E(r,\upsilon)\right|^2 rdr}{\int_0^\infty \left|E(r,\upsilon)\right|^2 rdr}$$

All emission and absorption cross sections included in the model are spectrally resolved. The spectral region from 1450 to 1650 nm has been subdivided into 2000 slots of $\delta\lambda = 0.2nm$. Propagation of the pump(s), and both ASE powers are described by the following propagation equations [12-14]:

$$\frac{dP_p(z)}{dz} = -\eta(\upsilon)\sigma_e(\upsilon)n_2(z)P_p(z)$$

$$\frac{dP_{ASE\pm}(z,\upsilon)}{dz} = \pm 2h\upsilon\Delta\upsilon\eta(\upsilon)\sigma_e(\upsilon)n_2(z) \pm [\sigma_e(\upsilon)n_2(z)-\sigma_a(\upsilon)n_1(z)]\eta(\upsilon)P_{ASE\pm}(z,\upsilon)$$

In accordance with the experimental setup schematically shown in Figure 1, appropriate boundary conditions are imposed at the beginning and at the end of the active fiber ($z = 0, l$) on the pump power and the individual spectral components of co- and counter directionally propagating ASE powers generated within the EDF. The boundary conditions are as follows,

$$P_P(0,\upsilon_p) = P_P$$

$$P^k_{ASE+}(0,\upsilon) = P^{k-1}_{ASE+}(L,\upsilon)F(\upsilon)\beta_{ring}$$

$$P^k_{ASE-}(0,\upsilon) = P^{k-1}_{ASE-}(L,\upsilon)F(\upsilon)\beta_{ring}\beta_{oi}$$

Where the upper index k at $P^k_{ASE+}(0,\upsilon)$ denotes the iteration step, β_{oi} is the isolation of the optical isolator and $F(\upsilon)$ is the relative transmittance of the optical bandpass filter, β_{ring} represents the total loss of the ring resonator and is composed of the losses of the optical

bandpass filter and the output coupler. An iterative solution of the rate equations and propagation equations for pump(s) and both the forward and backward propagating amplified spontaneous emission powers is implemented using a fourth-order Runge–Kutta routine.

In the following experiments and analysis, an Erbium-doped fiber with absorption coefficient of $\alpha(1530nm) = 6.3dB/m$, $\alpha(980nm) = 3.1dB/m$, of doping concentration of $5.9\times10^{24}\,\text{ions}/\text{m}^3$, of core diameter 1.92 μm , cutoff wavelength 1260 nm, and numerical aperture of 0.25 has been considered. Unless otherwise stated, a pump wavelength of 980 nm is assumed.

3.1 Effect of total intracavity loss

A deeply saturated EDF being able to offer wide-band and flat gain can be obtained by injection of a high power pump signal that is available in an EDFL by minimizing the total intracavity loss to keep as much laser power as possible in the cavity [8, 9]. Therefore, the total intracavity loss is the most important factor that influences the performance of a tunable EDFRL. We have investigated the effect of total intracavity loss on the EDFRL characteristics for different EDF lengths and various pump powers. In all the simulations, the coupling ratio of the output directional coupler was assumed constant and equal to 10%. Fig. 2 shows the output power as a function of emission wavelength for the intracavity losses of β_{ring} =3, 5, 7, and 9 dB, and with the EDF length of 7.5 m and a launched backward pump power of 200 mW. From Figure 2, we can see that both the laser output power and the tunable range are very sensitive to the intracavity loss. They increase significantly as is reduced, for 3 dB the EFRL can be tuned from 1488 to 1634 nm. This stresses the importance of minimizing the ring cavity loss if broad-band tuning is desired.

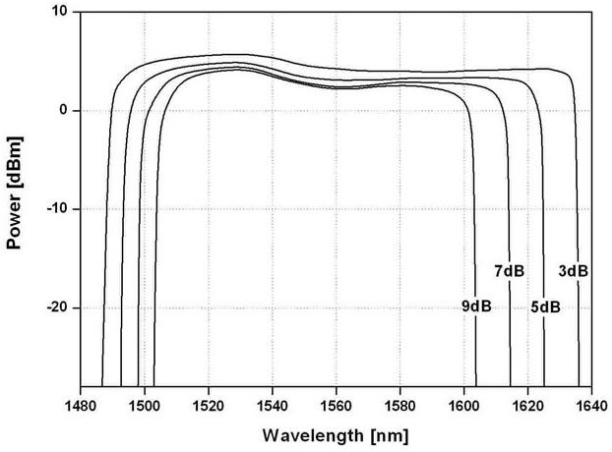

Fig. 2. Simulated output power versus wavelength for different ring cavity loss, P_p =50 mW, L = 7 m, γ =0.1, β_{ring} =3 dB, 5 dB, 7 dB, 9 dB.

3.2 Effect of erbium-doped fiber length

Fig. 3 shows the simulated output power versus the emission wavelength for P_p =50 mW, β_{ring} =3 dB, and γ_{out} =0.1 (the value of is the same as the measured value from the experimental setup) for various length of Erbium-Doped fiber of 3 m, 5 m, 7 m, 10 m, 15 m, 25 m. It can be seen from Figure 3 that, for the EDF length of 3 m, the tuning bandwidth is about 100 nm (1502-1602 nm) for 3 dB flatness. With an increase in the EDF length from 3 m to 7 m, the tuning range becomes broader, and the center wavelength shifts to the longer wavelength region. The tuning bandwidth reaches 147 nm covering the whole S+C+L band. For the EDF length longer than 12.5 m, the bandwidth and power decreases both rapidly. Finally, with an EDF length of 25 m, the bandwidth is only 76 nm (1527-1603 nm). It can be seen that optimization of the EDF length is necessary for achieving the largest tuning range and the high output power at the certain pump power. For 3 m long EDF, the output power decreases more rapidly in both shot wavelength region of C-band and long wavelength region of L-band due to the short gain media length to obtain sufficient gain. On the contrary, for 15 m and 25 m long EDF, the laser power decreases more rapidly in the C-band region below 1525 nm due to the self absorption of the long EDF. Thus, the range of 5-10 m long EDF can give the largest tuning range and the highest average power.

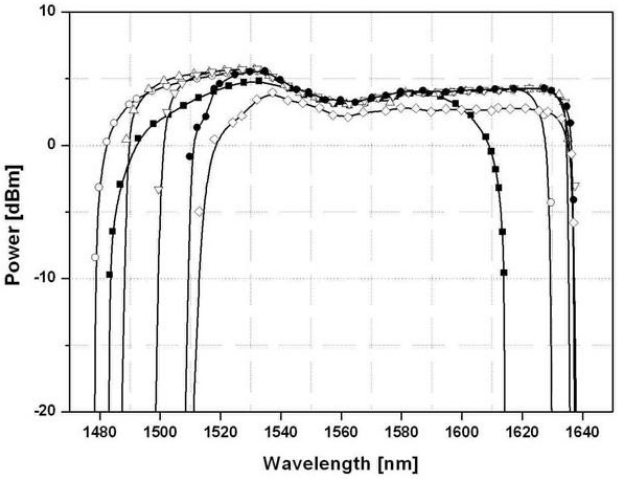

Fig. 3. Simulated output power versus wavelength for different EDF length, P_p =50 mW, γ_{out} = 0.1, β_{ring} =3 dB, L = 3 m(■), 5 m(○), 7 m(△), 10 m(▽), 15 m(●), 25 m(◇).

3.3 Effect of output coupling ratio

Output coupling ratio decided the ratio of light power inside the ring cavity, and influence the saturation of EDF. Fig. 4 shows the output power versus the emission wavelength for different values of γ_{out} =0.1, 0.3, 0.5, 0.7

with P_p =50 mW, L =7 m, β_{ring} =3 dB. A reduction in 3 dB bandwidth from 140 nm (1409–1632 nm) to 90 nm (1512–1602 nm) is observed when increasing from 0.1 to 0.7. However, the output power greatly increases in this case due to the increase. It can be seen from figure 4 that the optimal output coupling ratio varies in a large range with the emission wavelength, and an ultrabroad bandwidth can only be obtainable at a small value of output coupling ratio.

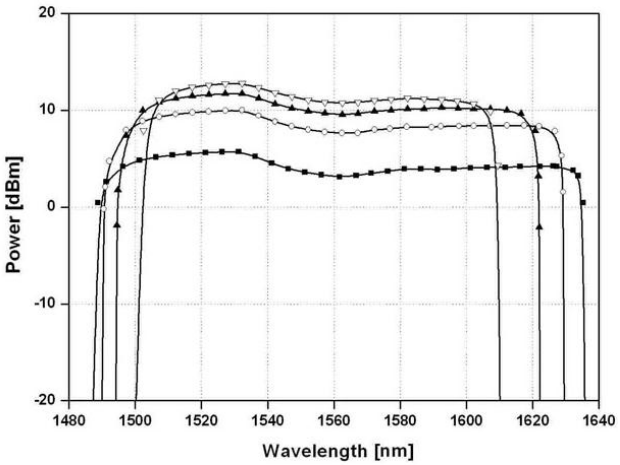

Fig. 4. Simulated output power versus wavelength for different output coupling ratio, P_p =50mW, L =7m, β_{ring} =3dB, γ_{out} =0.1(■), 0.3(○), 0.5(▲), 0.7(▽)

4. Results and discusions

The experimental setup of the tunable fiber ring laser is illustrated in Figure 1. The laser beam comes out of the ring cavity through one port of the output coupler and is measured by an optical spectrum analyzer (OSA, ANDO AQ6317C) and an optical power meter (PM, Anritsu MT9810B). The simulated results for the tunable range with P_p =50 mW, L =7 m, γ_{out} =0.1 are shown in Figure 5 (curves), together with the experimental data (points). Compared with the simulated results in Figure 5, the output power and bandwidth are reduced, especially in the cases of long EDF length. Small discrepancies may be because of the different intracavity losses arising from fusion splicing for different EDF lengths, as well as the limited tuning range of the tunable filter. Compared with the simulated results, the flatness of experimental data is better, this is because the theoretical simulation doesn't consider gain displacement phenomenon [14] that result in gain in L band smaller than actually.

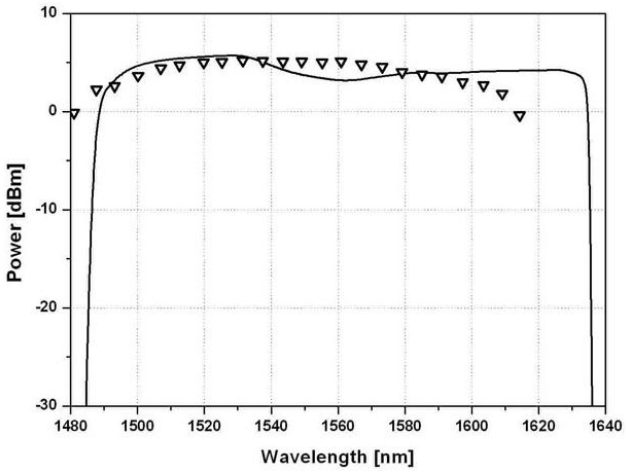

Fig. 5. Laser output power curve of experiment (▽) and simulation (-), P_p =50 mW, L =7 m, γ_{out} =0.1, β_{ring} =3 dB.

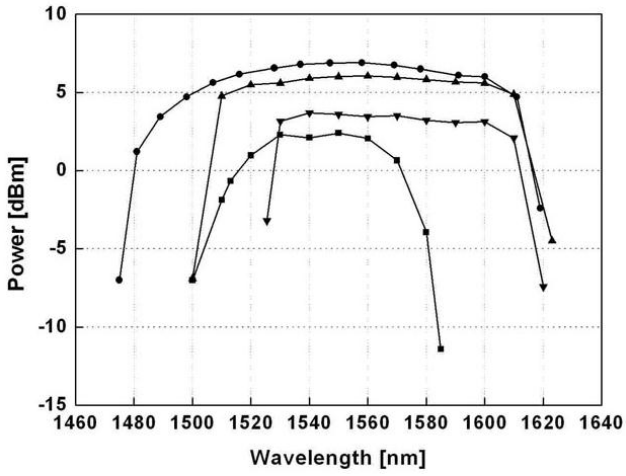

Fig. 6. The laser output power versus the emission wavelength for different EDF length, P_p =60 mW, γ_{out} =0.1, β_{ring} =3 dB, L=3 m (■), 7 m (●), 16 m (▲), 30 m (▼).

Fig. 6 illustrate the laser output power versus the emission wavelength for different EDF length L =3 m, 7 m, 16 m, 30 m with P_p =60 mW, γ_{out} =0.1, β_{ring} =3 dB. We can see from the figure that the results presented in figure indicate that the EDF length for optimal tuning range is about 5–10 m, in good agreement with the simulations results. The tuning range is 116 nm (1480–1616 nm) is achieved at EDF length of 7 m.

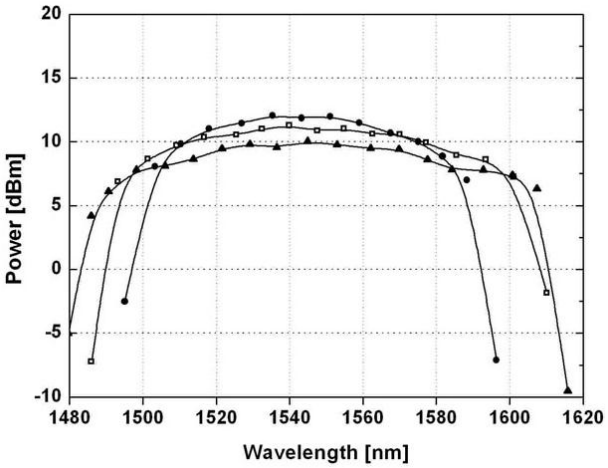

Fig. 7. The laser output power versus the emission wavelength for different output coupling ratio, P_p =50 mW, L =7 m, β_{ring} =3 dB, γ_{out} =0.3(▲), 0.5(□), 0.7(●).

Fig. 7 shows that the laser output power versus the emission wavelength for different output coupling ratio γ_{out} =0.3，0.5，0.7 with P_p =50 mW, L =7 m, β_{ring} =3 dB. We can see from the figure 7, as the increase of the output coupling ratio, tuning bandwidth becomes narrower and the output power greatly increases. This also accord with the theoretical model very well.

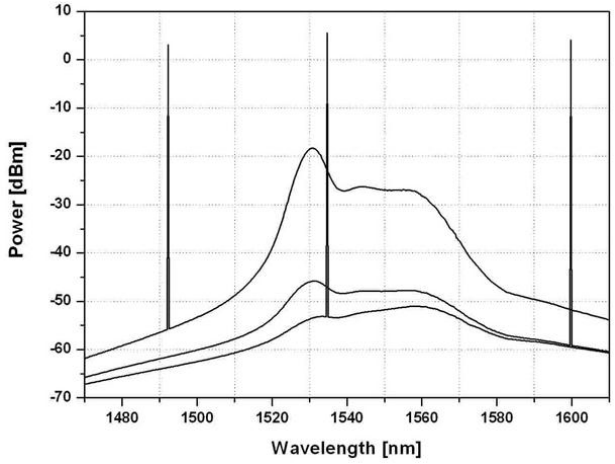

Fig. 8. Simulated laser output spectrum of the EDFRL, P_p =50 mW, L =7 m, β_{ring} =3 dB, γ_{out} =0.1, λ =1492 nm, 1535 nm, 1600 nm.

The simulated laser output spectra of the EDFRL for P_p =50mW, L =7m, β_{ring} =3dB and γ_{out} =0.1 for the three emission wavelengths λ =1492 nm, 1535 nm and 1600 nm are shown in Figure 8. From the figure, we have found that high C-band ASE noise arises when the laser emits at the short (less than 1530 nm) or the long (beyond 1600 nm) wavelength ends. High OSNR can only be expected in the center region of the tuning bandwidth.

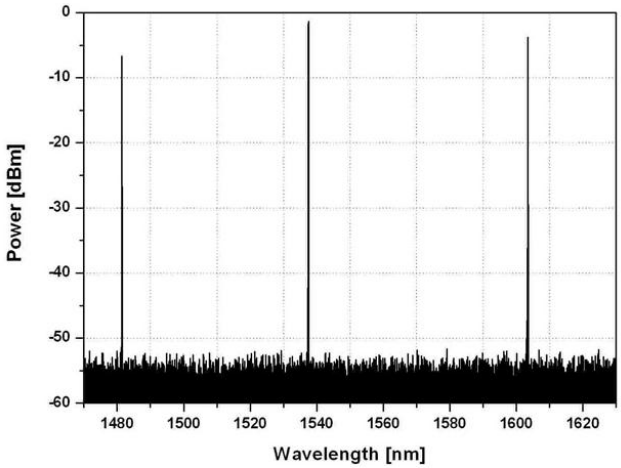

Fig. 9. The laser output spectrum of the EDFRL P_p =50 mW, L =7 m, β_{ring} =3 dB, γ_{out} =0.1, λ =1481 nm, 1537 nm, 1604 nm, resolution=0.01.

Fig. 9 shows the measured laser output spectra at three emission wavelengths λ =1481 nm, 1537 nm and 1604 nm. Because of the place of the tunable filter in front of output coupler, the ASE noise in the C-band is greatly suppressed and the OSNR is hence enhanced, especially for the laser emitting at the short or the long wavelength end where high OSNR better than 60 dB can be achieved.

5. Conclusions

This paper presents a broadband tunable erbium doped fiber ring laser (EDFRL) that can be continuously tuned 147 nm, covering the whole S and C+L bands from 1479 to 1616 nm. A comprehensive theoretical model for erbium-doped fiber ring lasers based on an iterative solution of propagation rate equations is used to analyze the dependence of laser output power characteristics on total intracavity loss, erbium-doped fiber length and output couple ratio. Numerical results, which are in good agreement with the experimental measurements, have indicated that minimization of the intracavity loss and optimization of the active fiber length and the output coupling ratio are extremely important for achieving good performance in an ultratunable EDFRL. It is worthwhile to note that for this laser configuration, a 1 dB increase in cavity loss decreases the tuning range by about 2 nm at the short wavelength end and by 5 nm at the long wavelength end. The optimized erbium-doped fiber length and output coupling ratio have been obtained through theoretical simulation and experimental study. This multilongitudinal mode laser offers a moderate coherence well suited for test and measurement applications. This ring fiber laser has simple configuration, low threshold, flat laser spectral distribution and high signal-to-ASE-noise ratio better than 60 dB.

Acknowledgements

This work was partly supported by the Fundamental Research Funds for the Central Universities (N090504002, N100404006), the National Natural Science Foundation of China (61074170), and the Specialized Research Fund for the Doctoral Program of Higher Education of China (20100042110029).

References

[1] S. Yamashita, M. Nishihara, Proc. 5th Asia–Pacific Conf. Communications and 4th Optoelectronics and Communications Conf., APCC/OECC'99, **2**, 1509 (1999).
[2] A. Bellemare, M. Karasek, C. Riviere, F. Babin, G. He, V. Roy, G. W. Schinn, IEEE J. Sel. Topics Quantum Electron., **7**, 22 (2001).
[3] X. Dong, N. Q. Ngo, P. Shum, H.-Y. Tam, X. Dong, Opt. Exp., **11**, 1689 (2003).
[4] X. Dong, H.-Y. Tam, B.-O. Guan, C.-L. Zhao, X. Dong, Opt. Commun., **224**(4–6), 295 (2003).
[5] S. Yamashita, M. Nishihara, Proc. 5th Asia-Pacific Conf. Communications/4th Optoelectronics Communications Conf. (APCC/OECC'99), **2**, 1509 (1999).
[6] A. Bellemare, M. Karasek, C. Riviere, F. Babin, G. He, V. Roy, G.W. Schinn, IEEE J. Selec. Top. Quantum Electron.. **7**, 22 (2001).
[7] S. Yamashita, M. Nishihara, IEEE J. Selec. Top. Quantum Electron..**7**, 41 (2001).
[8] Xinyong Dong, P.Shum, N.Q.Ngo, H.Y. Tam, Xiaoyi Dong, Journal of Lghtwave Technology, **23**(3), 1334 (2005).
[9] Wang, Qi, Yu, Qing-Xu, Guangdianzi Jiguang, Journal of Optoelectronics Laser, **17**, n SUPPL., 151 (2006).
[10] M. Karasek, J.A. Valles, J. Lightwave Technology, **16**, 1795 (1998).
[11] M. Karásek, A. Bellemare, Inst. Elect. Eng. Proc. Optoelectronics, **147**, 115 (2000).
[12] Paul F. Wysocki, M. J. F. Digonnet, B. Y. Kim, H. J. Shaw, "Characteristics of Erbium-Doped Superfluorescent Fiber Sources for Interferometric Sensor Applications," Journal of Lightwave Technology, **12**(3), 550 (1994).
[13] T. Georges, E. Delevaque, "Analytical modeling of high-gain erbium-doped fiber amplifiers," Opt. Lett. **17**, 1113 (1992).
[14] J. F. Massicott, J. R. Armitage, R. Wyatt et al. High gain broadband 1.6 μm Er3+ doped silica fiber amplifier [J]. Electron. Lett. **26**(20), 1645 (1990).

*Corresponding author: wangqi@ise.neu.edu.cn